Original Research Article

Nigerian Journal of Biotechnology and Life Sciences
ISSN: 2814-0281
Vol. 3 No 2c (2026) p. 661 - 669
http://www.njbls.fud.edu.ng/

Synthesis Generation and Optimization of Inorganic Saturable Absorbers in Pulsed Fiber Lasers for Medical Applications

N. M. Gidado[1]*, F. M. Umar[2], Z. I. Takai[2], H. Bawa[3], S. Gwadabe[1] and M. B. Isa[2]

[1]Department of Physiology Northwest University, Kano
[2]Department of Physics Northwest University, Kano
[3]Department of Human Physiology, Abubakar Tafawa Balewa University, Bauchi

*Corresponding Author: nmgidado@nwu.edu.ng

https://doi.org/10.67601/njbls.v3i2c.126

Article info
Date received
16/08/2026
Date accepted
26/09/2026
Available online
30/09/2026

Keywords
Q-switched, inorganic saturable absorbers, Figure-8 (FO8) cavity, fiber lasers

Abstract

This study presents the successful generation and optimization of the Q-switched pulsed fiber lasers by using a novel inorganic saturable absorber (SA) material of liquid and thin-film magnesium nitrate ($Mg(NO_3)_2$) in a Figure-8 (FO8) cavity design. The solid-state laser operated at a maximum repetition rate of 36.34 kHz, with a pulse width of 5.94 μs, a maximum pulse energy of 13.20 nJ and an average output power of 0.45 mW at 403 mW of pump power. In moving to the $Mg(NO_3)_2$ thin-film configuration, the performance was greatly improved allowing the repetition rate to be tuned from 35.36 kHz to 72.56 kHz and the pulse duration to be shortened from 4.240 μs to 3.005 μs with increasing pump power from 154.3 mW to 403.00 mW. Moreover, the system could be made to be wavelength tunable with stable operation throughout the 30 nm tuning range (1525 nm to 1555 nm) with a fixed pump power of 403 mW by incorporating a tunable bandpass filter to the cavity. The findings reinforce the potential of the controlled integration and optimization of inorganic $Mg(NO_3)_2$ SAs to realize high reliability and highly tunable pulsed fiber laser sources for advanced medical applications.

Introduction

The outstanding beam quality, compact size, and efficient thermal management have made them essential tools in a wide range of high-tech applications, including advanced medical diagnostics, surgical and dermatological applications (Gambling 2000). The most basic design elements for achieving short-pulsed regimes of operation in lasers, like Q-switching and mode locking, are optical switches called saturable absorbers (SAs) (Ibarra-Escamilla et al., 2008). SAs allow for the delivery of intensity-dependent transmission which enables the production of high-peak-power, microsecond to femtosecond pulses, necessary for precision medical applications such as tissue ablation, ophthalmology, and microsurgery (Gao et al., 2009). This is currently occupied by Semiconductor Saturable Absorber Mirrors (SESAMs) which have the drawbacks of narrow operation bandwidths, complicated fabrication processes and high production costs (Garmire 2000). Therefore, recent studies have shifted focus to new low dimensional-type inorganic materials and compounds, such as

Copyright: ©2026 the Author(s). Published by Federal University Dutse. This is an open-access article distributed under the terms of the Creative Commons Attribution 4.0 International License (CC BY 4.0).

transition metal dichalcogenides, topological insulators and metal oxides, as new advanced saturable absorbers (Going et al., 2012). Thanks to their large absorption bandwidths, extremely fast recovery times and great environmental stability, these inorganic materials are ideal candidates for the use in demanding medical grade laser systems as compared to organic dyes or traditional semiconductor counterparts (Gokus et al., 2009).

Although inorganic saturable absorbers have shown outstanding photophysical characteristics, they have been so far scarcely embraced in pulsed fiber lasers for medical applications because of several major problems related to their synthesis, generation and optimization (Guo et al., 2016). The current synthesis techniques provide a large number of synthesis defects, such as non-uniform film thickness, high defect density, and poor batch to batch reproducibility, which directly impact stable mode locking and long-term laser reliability (Hakulinen et al., 2025).

A high modulation depth with high clinical power operation for inorganic SAs while keeping a high optical damage threshold is a tough engineering challenge (Hakulinen et al., 2024). The losses often involved with the effective integration of these materials onto fiber tips, tapered fibers or side polished fibers can lead to high insertion losses and scattering losses, thus reducing the overall Q-factor and output efficiency of the cavity (Huang et al., 2020). However, there is a lack of standardization and scalability in frameworks that guarantee the performance of these inorganic SAs under the strict duty cycles that are typical to medical environments (Ibarra-Escamilla et al., 2014).

Such systematic synthesis, controlled generation and cavity optimization of pulsed fiber laser technologies is crucial to overcome these bottlenecks to enable the transition of material science advancements to reliable, clinically-ready pulsed fiber laser technologies (Huang et al., 2020). In the present work, these challenges have been addressed and the performance and reliability of fiber lasers employing organic and inorganic SAs have been increased for medical applications.

Methodology

The magnesium nitrate ($Mg(NO_3)_2$ was prepare using solution casting method as showing below, the polyvinyl alcohol (PVA) was dissolved in 1 ml of distilled water and stirred continuously for the entire night until a uniform white solution was obtained. Then, the $Mg(NO_3)_2$ powder was added into the PVA solution and stirred vigorously under magnetic stirrer for 60 minutes at 100°C, as revealed in Figure 1 below. The solution attained homogeneity as the $Mg(NO_3)_2$ powerfully dissolved, resulting in a white coloration. After cooling at room temperature, the $Mg(NO_3)_2$ solution was divided into three samples with different concentrations: 50/50, 70/30, and 80/20 to form a thin film as shown in Figure 1 (c). The $Mg(NO_3)_2$solution based polymer was poured into pteri dish for drying process at temperature of 60 and duration of 24 hours, aligning with a similar trend reported by (Al-Hayali et al., 2017).

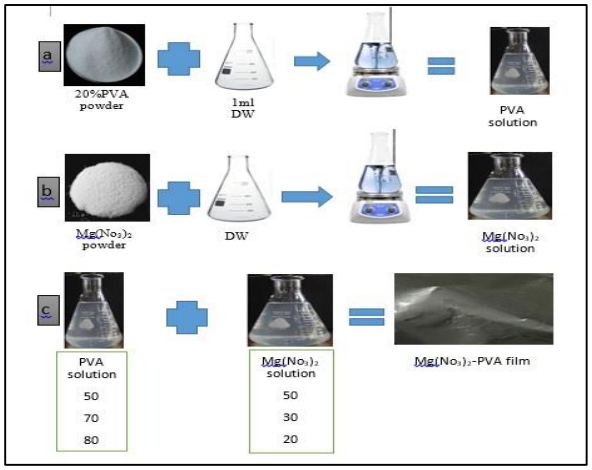


Figure 1: Preparation of $Mg(NO_3)_2$ solution and the SA film

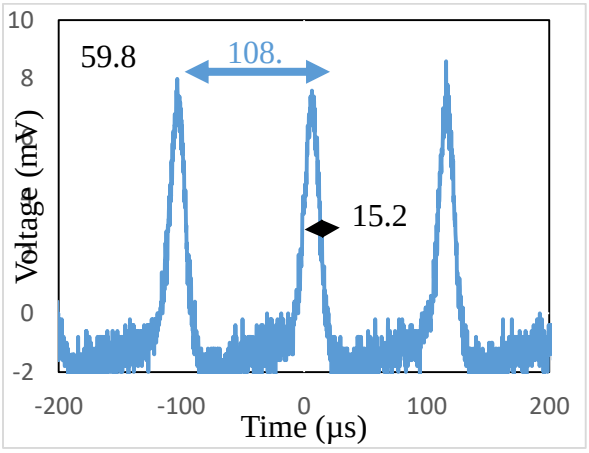
Results and discussion

Generation of Q-switching using liquid Magnesium Nitrate

The Q-switching phenomenon was successfully demonstrated through the utilization of liquid $Mg(NO_3)_2$. This innovative approach showcased the effective generation and control of Q-switched pulses in the fiber laser system, adding a novel dimension to the field of laser technology. The use of liquid $Mg(NO_3)_2$as an SA highlights its potential for enhancing the versatility and performance of

fiber laser devices, contributing valuable insights to the ongoing exploration of advanced laser applications (Gao et al., 2009).

Figure 2 (a) displays a typical pulse train of Q-switched pulse fiber laser at minimum pump power of 59.8 mW with pulse duration of 15.25 µs and period of 108.80 µs. Meanwhile, Figure 2 (b) exhibits the pulse train at maximum pump power of 403.00 mW with period of 28 µs and narrow pulse width of 6.60 µs (Javan et al., 2013). The pulse trains maintained a constant intensity distribution with no discernible variation or amplitude modulation. This demonstrates the pulse regime's stability and capacity to function at different repetition rates and pulse widths (Geisari & Kalnins, 2016).



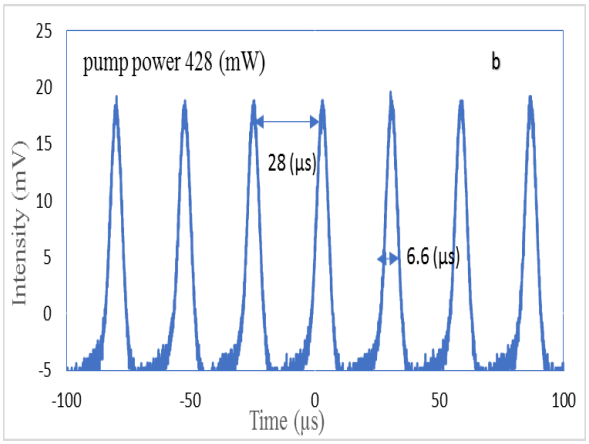


Figure 2: A typical oscilloscope trace of Q-switched EDFL with LMg(NO₃)₂-SA at a) 59.8 & b) 428 mW pump power.

Figure 3 illustrates the Q-switched spectrum, which exhibits a central wavelength of 1553 nm, a resolution of 1.0 nm, and an output power of -7.9 dB. Several peaks can be seen in the optical spectrum because of mode competition and a greater cavity length in the FO8 designs. This is the situation since the cavity length is longer (Giakos et al., 2004). This competition mode was created due to a uniform gain broadening in EDF. However, it can be mitigated with the help of the inhomogeneous loss features of nonlinear polarisation rotation (NPR), which causes intensity-dependent loss for various frequencies. Thus, the multiple peaks are exhibited to balance the effect of mode competition of EDF as well as inhomogeneous loss caused by NPR (Huang et al., 2020).

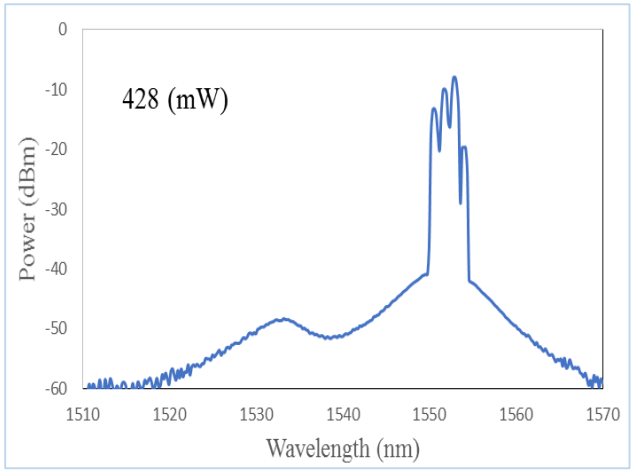


Figure 3: Output spectrum of Q-switched EDFL with LMg(NO₃)₂-SA at pump power of 428 mW.

The Figure 4 shows the relationship between repetition rate and pulse width against pump power. When tuning the pump power, the repetition rate of Q-switched pulse fiber laser rises continuously from 9.19 kHz to 36.34 kHz. In the meantime, the pulse width dramatically declines from 15.25µsto 5.94 µs.The reduction in pulse width and the simultaneous increase in the repetition rate with rising pump power represent characteristics of passive Q-switching (Gui et al., (2011).

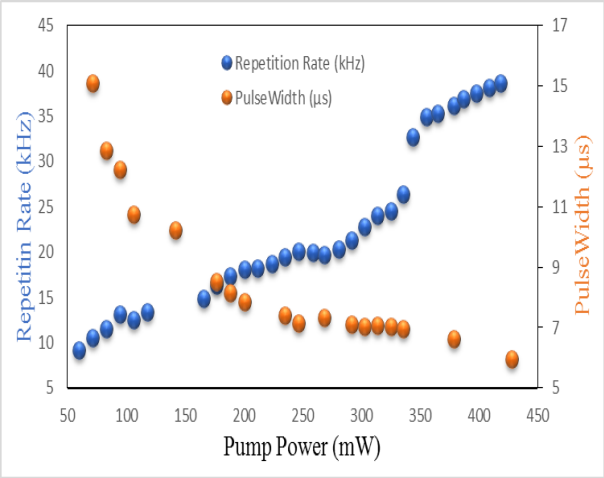


Figure 4: Repetition rate and pulse width as functions of pump power of Q-switched EDFL with liquid $Mg(NO_3)_2$ SA.

Figure 5 presents the pulse energy and the average output power against the pump power. The average output power increases from 0.031 mW to 0.45 mWby increasing the pump power from 154.3 mW to 403 mW. Meanwhile, the calculated pulse energy grew from 1.16 nJ to 13.20 nJ when changing the pump power from 154.3 mW to 403 mW similar trend was reported by González et al. (1996).

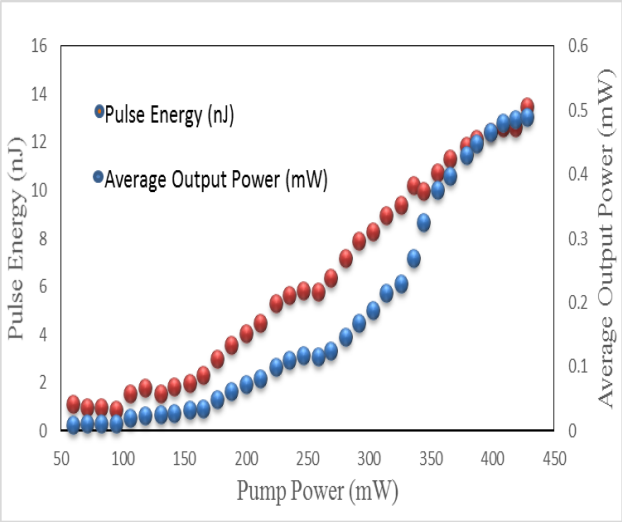


Figure 5: Output power and pulse energy of Q-switched EDFL with liquid $Mg(NO_3)_2$-SA versus the input pump power.

Then, the stability of the pulse was investigated from the OSC, as illustrated in Figure 4.38. The resolution bandwidth and span from the OSC are 100 kHz and 100 Hz, respectively (Goulielmakis et al., 2008). The fundamental frequency is precisely synchronised with the Q-switched pulse repetition rate of 36.9 kHz. Regarding the SNR, the fundamental frequency has a value of 52.3dB. The SNR is more significant than 50.00 confirm the stability of Q-switched pulse fiber laser (Gui et al., 2011).

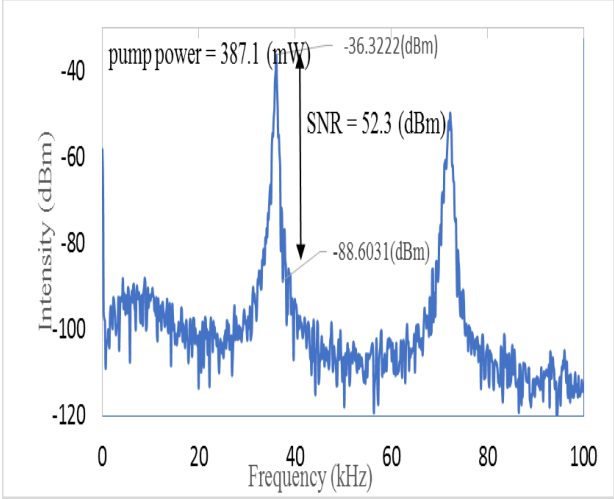


Figure 6: RF spectrum of Q-switched EDFL with $Mg(NO_3)_2$-SA at pump power of 387.1 mW with 36.9 kHz repetition rate.

Generation of Q-switched using magnesium nitrate film

The generation of Q-switched pulse fiber laser was investigated by inserting $Mg(NO_3)_2$thin film inside FO8 cavity. After the incorporation of $Mg(NO_3)_2$ thin film, it is possible to observe the self-starting Q-switched pulse fiber laser functioning at pump power of 154.3 mW. Figure 7 shows the typical pulse train of Q-switched pulse fiber laser at different pump power. Figure 7 (a) the pulse train at minimum pump power of 154.3 mW with pulse width of 4.240 µs and the period of 28.00 µs. Meanwhile, the pulse width was reduced to 3.005 µs with period of 29.34 µs when the pump power rising to 403.00 mW (Gui et al., 2011).

Further increasing the pump power above 403.00 mW shows an irregular Q-switched pulse, and the pulse is stable when the pump power in between 154.30 mW to 403.00 mW. These phenomena indicated the $Mg(NO_3)_2$ thin film did not experience damage of SA (Guy et al., 1994). The oversaturation

of the $Mg(NO_3)_2$ thin film under high incident intensity leads to instability in the Q-switched state. The $Mg(NO_3)_2$ thin film undergoes a process that is associated with two-photon absorption, which was triggered by the presence of high optical intensity (Haiml et al., 2004). Consequently, the absorption coefficient escalates as the pump power steadily climbs. Thus, the Q-switched operation was impossible to proceed when the pump power exceeds 403.00 mW. The $Mg(NO_3)_2$ thin film was removed from the laser cavity to examine the state of the Q-switched pulse. The findings demonstrate that only a continuous-wave was observed on the OSA and OSC, providing evidence that a Q-switched pulse fiber laser can be created with the assistance of a thin film of $Mg(NO_3)_2$ (Hakulinen & Okhotnikov 2007).

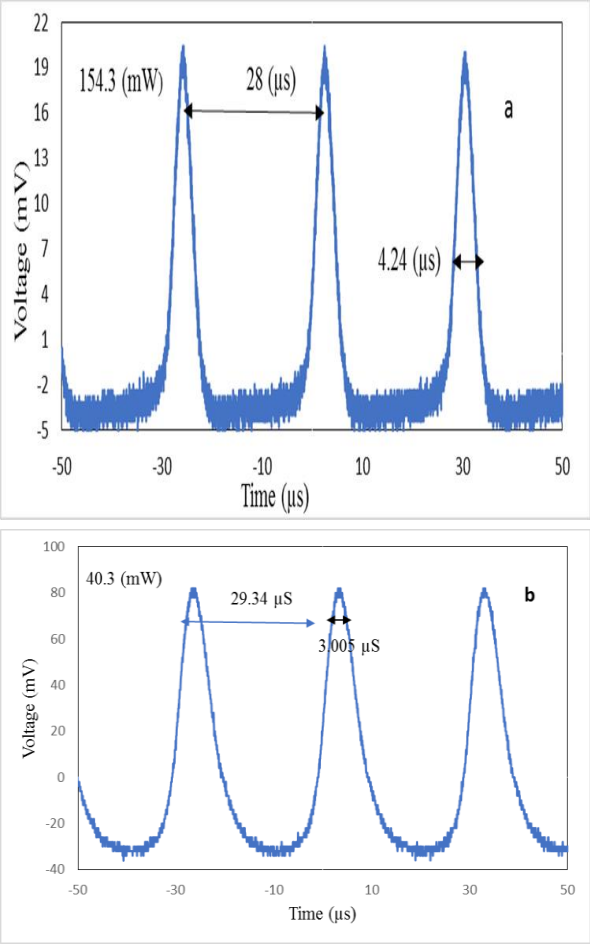


Figure 7: Typical pulse trains for the proposed EDFL configured with a $Mg(NO_3)_2$- film SA at a pump power a) threshold 154.3 mW, and b) maximum 40.3 mW.

When changing the pump power, the repetition rate of the Q-switched pulse fiber laser increases steadily from 35.36 kHz to 72.56 kHz. Meanwhile, as depicted in Figure 8, the pulse duration significantly decreased from 4.240µs to 3.005µs (Hamdalla & Hanafy 2016). This occurs because the pump power was increased, leading to a higher number of photons being circulated within the FO8 cavity. As a result, the $Mg(NO_3)_2$ thin film becomes saturated. Thus, by increasing the modulation depth of the $Mg(NO_3)_2$ thin film and optimizing the design of the fiber laser cavity, it is possible to achieve a further reduction in the pulse width of the Q-switched pulsefiber laser (Hammadi et al., 2018).

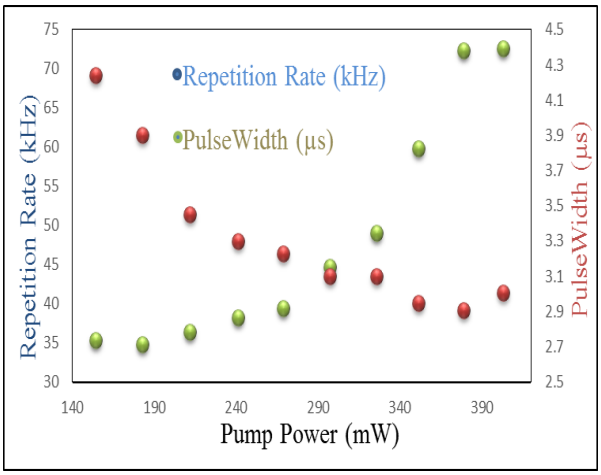


Figure 8: Repetition rate and pulse duration relationships with pump power for $Mg(NO_3)_2$ film SA.

Figure 9, illustrates the relationship between pump power, pulse energy and average output power in the Q-switched pulse fiber laser. According to the figure, the pulse energy exhibited a rise from 0.877 nJ to 6.200 nJ as the pump power was altered from 154.3 mW to 403.00 mW. The average slope has an efficiency of 0.022 as reported by Harun et al. (2015). Simultaneously, the average output power also demonstrated in increase from 0.031 mW to 0.450 mW when the pump power was changed from 154.3 mW to 403.00 mW with slope efficiency of 0.0017 (Hasan et al., 2009).

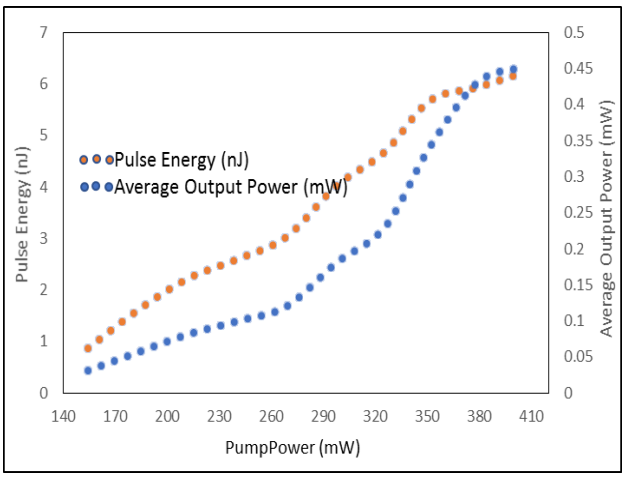


Figure 9: Pulse energy and average output power against pump power.

Figure 10 displays the RF spectrum with resolution bandwidth of 0.1 kHz. The data was obtained at a fundamental frequency of 36.1 kHz, showcasing a SNR of 52.3 dB (Hasegawa & Kodama 1990). The SNR value more than 50 dB indicates the stable performance of Q-switched pulse fiber laser similar with the SNRs of the metal oxides transition such as zinc oxide (Harun et al., 2015) and graphene (Gui et al., 2011).

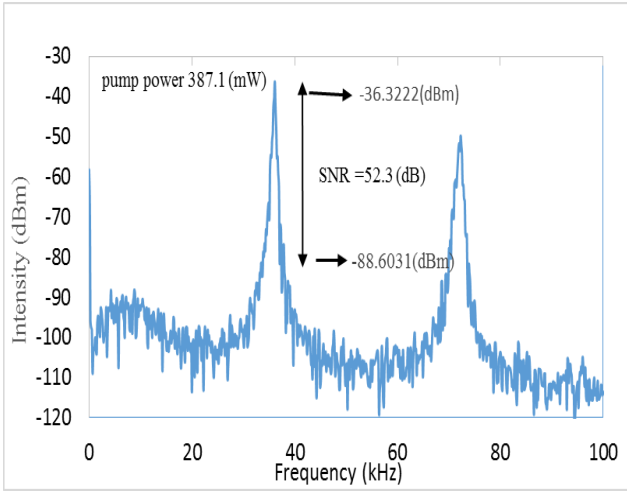


Figure 10: RF spectrum at pump power of 387.1 mW.

Tunable Q-switched pulse fiber laser using magnesium nitrate

The stable Q-switched pulse fiber laser at the pump power of 403.00 mW was observed for the wavelength tunability by incorporating TBF inside FO8 cavity design and $Mg(NO_3)_2$ thin film as SA Haus (1975). Figure 11 presents the output spectra of the tunableQ-switched pulse fiber laser for 4 tuned wavelengths. The wavelength was recorded from the OSA at an interval of 10 nm at pump powerof403.00mW. A wide wavelength range of 30nm was covered from 1525 nm to 1555 nm (He et al., 1998).

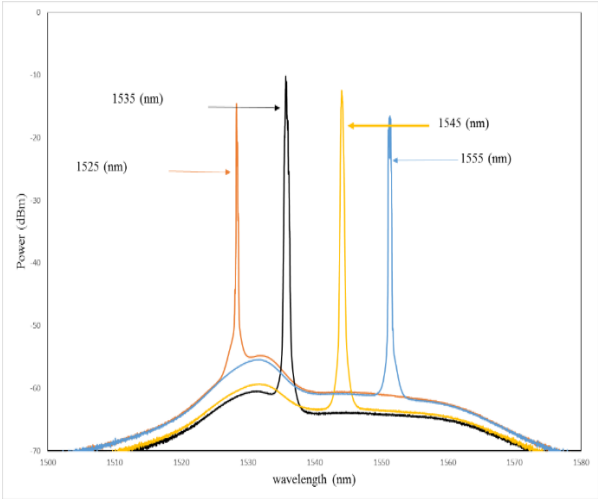


Figure 11: Output spectra of the wavelength tunable $Mg(NO_3)_2$-based Q-switched EDFL recorded at wavelength intervals of 10 nm.

Figure 12, displays the graph of the output pulse train from a tunableQ-switched pulse fiber laserat pump power of 403 mW, output wavelength of 1555 nm, and repetition rate of 72.56 kHz.

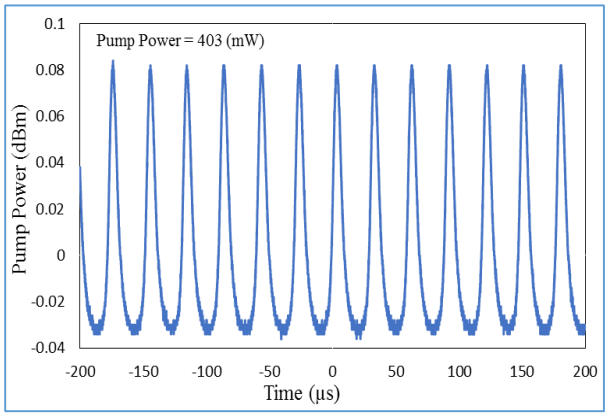


Figure 12: Output pulse train of the $Mg(NO_3)_2$-based tunable.

In addition, the tuning of the TBF allows for the investigation and reporting of the changes in repetition rate at different wavelengths, as shown

in Figure 13. The repetition rate varies significantly between 35.36 kHz and 72.56 kHz as the laser's wavelength was changing between 1525 and 1555 nm (Herda et al., 2005). This clearly explains that the intracavity laser is more powerful, and $Mg(NO_3)_2$ thin film bleaching occurs more quickly under quicker population inversion/depletion at alarger-gain EDF wavelength, occasioning in a higher repetition rate. No Q-switched pulse was observed beyond the tuning wavelength, showing the constraint on stable wavelength tenability (Hideur et al., 2001).

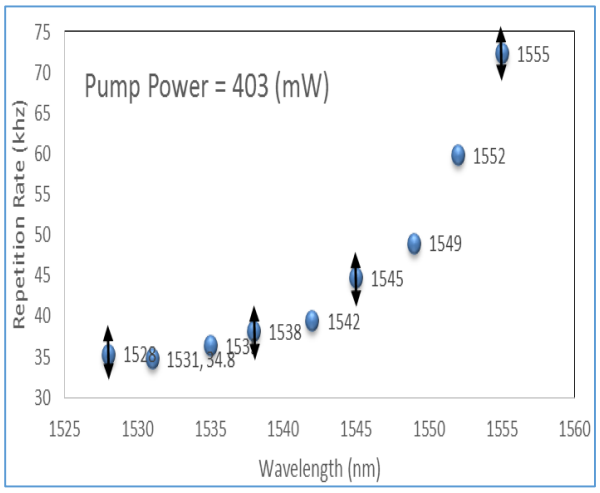


Figure 13: Repetition rate as a function of wavelength.

Conclusion

The Q-switched pulse fiber laser also can be generated when the liquid $Mg(NO_3)_2$ was implemented in FO8 cavity, which having a maximum repetition rate of 36.34 kHz, narrow pulse width of 5.94 μs, maximum pulse energy of 13.20 nJ, average output power of 0.45 mW at maximum pump power of 403 mW. Meanwhile, high repetition rate of Q-switched pulse fiber laser was demonstrated when the $Mg(NO_3)_2$ thin film was integrated inside the FO8 cavity design. When changing the pump power from 154.3 mW to 403.00 mW, the repetition rate was tuning from 35.36 kHz to 72.56 kHz while, the pulse duration decreased from 4.240 μs to 3.005 μs.

The performances of Q-switched pulse fiber laser were analyzed as tunable laser source using $Mg(NO_3)_2$ thin film as SA. The experimental setup was improved to become the Q-switched wavelength tunability based on the FO8 cavity by employing the tunable band pass filter as wavelength selective element. The tunable Q-switched pulse fiber laser operates from 1525 to 1555 nm with tunable range of 30 nm. The generated output pulses demonstrate a repetition rate ranging from 35.36 kHz to 72.56 kHz at fixed pump power of 403 mW. Thus, the integration, degradation, and optimization of organic and inorganic SAs had potential to generate pulsed fiber lasers for medical applications.

Acknowledgments

This work was financially supported by Northwest University, Kano, Nigeria under the Institutional Based Research Grand (IBR) funded by Tertiary Education Trust Fund (Tetfund). While preparation and characterization of the material was carryout at Microelectronic and Nanotechnology-Shamsuddin Research Centre (Mint-SRC) Universiti Tun Hussein Onn Malaysia (UTHM).

Author contribution

NMG and FMU: Conceptualization, methodology, experimental design, and original draft preparation. **ZIT and MBI:** Data curation, formal analysis, and investigation of the saturable absorbers. **HB and SG:** Validation, visualization, and manuscript review & editing. **NMG and ZIT:** Supervision, resources management, project administration, and final review

Conflict of Interest

The authors declare that they have no known competing financial interests or personal relationships that could have appeared to influence the work reported in this paper.

References

Gambling, W. A. (2000). The rise and rise of optical fibers. *IEEE journal of selected topics in quantum electronics*, *6*(6), 1084-1093. https://doi.org/10.1109/2944.902157

Gao, W., Alemany, L. B., Ci, L., & Ajayan, P. M. (2009). New insights into the structure and reduction of graphite oxide. *Nature Chemistry*, *1*(8), 403–408. https://doi.org/10.1038/nchem.281

Gao, X., Jang, J., & Nagase, S. (2009). Hydrazine and thermal reduction of graphene oxide: Reaction mechanisms, product structures, and reaction design. *Journal of Physical Chemistry C*, *114*(2), 832–842. https://doi.org/10.1021/jp909284g

Garmire, E. (2000). Resonant optical nonlinearities in semiconductors. *IEEE Journal on Selected Topics in Quantum Electronics*, *6*(6), 1094–1110. https://doi.org/10.1109/2944.902158

Geisari, N., & Kalnins, M. (2016). Poly (vinyl alcohol)-poly (vinyl acetate) composite films from water systems: formation, strength-deformation characteristics, fracture. In *IOP Conference Series: Materials Science and Engineering*, *111*(1), 012009. IOP Publishing.

Giakos, G. C., Molhokar, A., Orozco, A., Kumar, V., Sumrain, S., Mehta, D, Medithe, A. (2004). Laser imaging through scattering media. *Conference Record - IEEE Instrumentation and Measurement Technology Conference*, *1*, 433–437. https://doi.org/10.1109/IMTC.2004.1351081

Going, R., Popa, D., Torrisi, F., Sun, Z., Hasan, T., Wang, F., & Ferrari, A. C. (2012). 500 fs wideband tunable fiber laser mode-locked by nanotubes. *Physica E: Low-Dimensional Systems and Nanostructures*, *44*(6), 1078–1081.

Gokus, T., Nair, R. R., Bonetti, A., Bohmler, M., Lombardo, A., Novoselov, K. S., ... & Hartschuh, A. (2009). Making graphene luminescent by oxygen plasma treatment. *ACS nano*, *3*(12), 3963-3968.

González, J., Guinea, F., & Vozmediano, M. A. H. (1996). Unconventional quasiparticle lifetime in graphite. *Physical Review Letters*, *77*(17), 3589–3592. https://doi.org/10.1103/PhysRevLett.77.3589

Goulielmakis, E., Schultze, M., Hofstetter, M., Yakovlev, V. S., Gagnon, J., Uiberacker, M., ... & Kleineberg, U. (2008). Single-cycle nonlinear optics. *Science*, *320*(5883), 1614-1617.

Gui, L., Zhang, W., Li, X., Xiao, X., Zhu, H., Wang, K., ... & Yang, C. (2011). Mode-locked operation of an erbium-doped fiber laser using a self-assembled graphene membrane after excitation of Q-switched pulse. In *The European Conference on Lasers and Electro-Optics* (p. JSII1_5). Optica Publishing Group.

Guo, C., Chen, B., Wang, H., Zhang, X., Wang, J., Wu, K., & Chen, J. (2016). Investigation on the stability of WSe 2-PVA saturable absorber in an all PM Q-switched fiber laser. *IEEE Photonics Journal*, *8*(5), 1-12.

Guo, H. L., Wang, X. F., Qian, Q. Y., Wang, F. B., & Xia, X. H. (2009). A green approach to the synthesis of graphene nanosheets. *ACS nano*, *3*(9), 2653-2659. https://doi.org/10.1021/nn900227d

Guy, M. J., Noske, D. U., Boskovic, A., & Taylor, J. R. (1994). Femtosecond soliton generation in a praseodymium fluoride fiber laser. *Optics letters*, *19*(11), 828-830.

Haiml, M., Grange, R., & Keller, U. (2004). Optical characterization of semiconductor saturable absorbers. *Applied Physics B*, *79*, 331-339.

Hakulinen, T., & Okhotnikov, O. G. (2007). 8 ns fiber laser Q switched by the resonant saturable absorber mirror. *Optics letters*, *32*(18), 2677-2679. https://doi.org/10.1364/OL.32.002677

Hamdalla, T. A., & Hanafy, T. A. (2016). Optical properties studies for PVA/Gd, La, Er or Y chlorides based on structural modification. *Optik*, *127*(2), 878-882.

Hammadi, Y., Mansour, T. S., Alani, I. A. M., Ahmed, M. H. M., Al-Masoodi, A. H. H., Jusoh, Z., & Harun, S. W. (2018). Graphene based soliton mode-locked erbium doped fiber laser for supercontinuum generation. *Digest Journal of Nanomaterials and Biostructures*, *13*(3), 777-784.

Harun, S. W., Sabran, M. B. S., Azooz, S. M., Zulkifli, A. Z., Ismail, M. A., & Ahmad, H. (2015). Q-switching and mode-locking pulse generation with graphene oxide paper-based saturable absorber. *The Journal of Engineering*, *2015*(6), 208–214. https://doi.org/10.1049/joe.2014.0321

Hasan, T., Sun, Z., Wang, F., Bonaccorso, F., Tan, P. H., Rozhin, A. G., & Ferrari, A. C. (2009). Nanotube–polymer composites for ultrafast

photonics. *Advanced materials*, *21*(38-39), 3874-3899.

Hasegawa, A., & Kodama, Y. (1990). Guiding-center soliton in optical fibers. *Optics letters*, *15*(24), 1443-1445.

Haus, H. (1975). Theory of mode locking with a slow saturable absorber. *IEEE Journal of Quantum Electronics*, *11*(9), 736-746.

Haus, H. A. (1975). Theory of mode locking with a fast saturable absorber. *Journal of Applied Physics*, *46*(7), 3049–3058. https://doi.org/10.1063/1.321997

He, H., Klinowski, J., Forster, M., & Lerf, A. (1998). A new structural model for graphite oxide. *Chemical physics letters*, *287*(1-2), 53-56.

Herda, R., Okhotnikov, O. G., Rafailov, E. U., Sibbett, W., Crittenden, P., & Starodumov, A. (2005). Semiconductor quantum-dot saturable absorber mode-locked fiber laser. *IEEE Photonics Technology Letters*, *18*(1), 157-159.

Hideur, A., Chartier, T., Brunel, M., Salhi, M., Özkul, C., & Sanchez, F. (2001). Mode-lock, Q-switch and CW operation of an Yb-doped double-clad fiber ring laser. *Optics Communications*, *198*(1–3), 141–146. https://doi.org/10.1016/S0030-4018(01)01485-7

Huang, L., Zhang, Y., & Liu, X. (2020). Dynamics of carbon nanotube-based mode-locking fiber lasers. *Nanophotonics*, *9*(9), 2731-2761.

Ibarra-Escamilla, B., Kuzin, E. A., Duran-Sanchez, M., Pottiez, O., & Haus, J. W. (2014, November). Symmetric nonlinear optical loop mirror used as saturable absorber in mode-locked fiber laser. In *Latin America Optics and Photonics Conference* (pp. LTu1A-3). Optica Publishing Group.

Ibarra-Escamilla, B., Pottiez, O., Kuzin, E. A., Haus, J. W., Grajales-Coutiño, R., & Zaca-Moran, P. (2008). Experimental investigation of self-starting operation in a F8L based on a symmetrical NOLM. *Optics Communications*, *281*(5), 1226–1232. https://doi.org/10.1016/j.optcom.2007.10.075

Iijima, S. (1991). Helical microtubules of graphitic carbon. *Nature*, *354*(6348), 56-58. https://doi.org/10.1038/354056a0

Javan, A., Bennett Jr, W., & Herriott, D. (2013). Population inversion and continuous optical maser oscillation in a gas discharge. *Essentials of Lasers: The Commonwealth and International Library: Selected Readings in Physics*, *167*. https://doi.org/10.1016/B978-0-08-013320-1.50020-8